A Mechanobiological Framework for the Prediction of In-Stent Restenosis; Insights into the role of load induced damage in restenotic growth

David R. Nolan[1,2*], Caitríona Lally[1,2]

1. *Trinity Centre for Bioengineering, Trinity Biomedical Sciences Institute, Trinity College Dublin, Dublin, Ireland.*

2. *Department of Mechanical and Manufacturing Engineering, School of Engineering, Trinity College Dublin, Dublin, Ireland.*

* Email: dnolan4@tcd.ie, lallyca@tcd.ie

1. Introduction

Stents are commonly used worldwide for the treatment of atherosclerosis, with over one million procedures performed annually in the U.S. alone [0]. The problem of in-stent restenosis occurs post stent implantation whereby excessive migration and proliferation of vascular smooth muscle cells (VSMCs) decreases lumen cross-sectional area [2]. There is a strong correlation between the degree of stent arterial injury, and the resultant decrease in lumen area [2,3]. Therefore stent designs must strive to induce as little injury to the artery as possible. The advent of drug eluting stents has decreased cases of in-stent restenosis [4], however the optimum stent design still remains an open question [3,4,5].

In order to improve stent designs and minimise in-stent restenosis, it is critical to obtain a thorough understanding of the mechanobiology of arterial tissue, i.e. how arterial tissue responds to changes in mechanical state. After stent deployment, quiescent, contractile VSMCs are believed to change their phenotype to proliferative, synthetic VSMCs. These synthetic cells migrate to the lumen and form a restenotic lesion [3,6]. Damage to the surrounding extracellular matrix (ECM) has been shown to effect changes on VSMC phenotype and activation [7]. Matrix-degrading metalloproteinases (MMPs) degrade collagen in the ECM and have also been shown to regulate VSMC behaviour [8]. Variations in mechanical strain, which occur in stenting, can upregulate MMPs and lead to degradation of ECM [9]. Hence there is a complex, dynamic relationship between the mechanical environment caused by stenting, and the response of arterial tissue and its constituent VSMCs.

This paper presents an in silico mechanobiological model of in-stent restenosis. Whilst stent induced vascular injury has been extensively identified as the predominant stimulus for subsequent synthetic VSMC proliferation and restenotic neo-intimal growth [6], the specific mechanical stimulus analogous to this vascular injury has remained in question. In fact, mechanobiological models driven by different mechanical stimuli, such as von Mises stress [10] and cyclic damage accumulation [10], have been shown to successfully capture the key characteristics of restenosis post-stenting.

The specific aim of this work is therefore to directly compare these different damage models with a view to gaining greater insights into the mechanism of injury within stented vessels and the key role this plays in the progression of in-stent restenosis.

2. Materials and Methods

A coupled simulation environment is developed consisting of two primary components, namely (i) a continuum mechanical model solved using finite element (FE) analysis and (ii) an agent-based model (ABM) which explicitly models the behaviour of VSMCs and endothelial cells (EC) in the artery wall. In both components, a quarter symmetry idealised geometry of an artery is modelled. The FE model is used to determine the deformation and stresses in a vessel wall under a prescribed loading whilst the ABM simulates VSMC and EC behaviours such as phenotype change, migration and proliferation.

Two approaches are used to model how mechanical damage affects the behaviour of the ECM and the VSMCs; a stress magnitude approach (Model A), and a cyclic stress approach (Model B). The performance of these two models is assessed through the simulation of two common vascular interventions; initially a balloon angioplasty procedure is used to calibrate the damage – ECM dynamics, and subsequently each of the calibrated models are used to simulate stent deployment.

2.1 Continuum Mechanical Model

An FE model of a 2D quarter coronary artery is created, with the appropriate symmetry boundary conditions. An internal pressure is applied, corresponding to physiological pressures. Both media and adventitial layers are modelled discretely using a non-linear hyperelastic Ogden constitutive model, with a media to adventitia thickness ratio of 1.67 [10]. For details of the precise geometry and material parameters refer to [10].

2.2 Agent Based Model of Cell Activity

An ABM framework inspired by [12] is developed in Matlab (R2015b, Natick, MA). Cells are explicitly modelled as contact inhibited spheres/circles. VSMCs are seeded randomly within the artery wall at a density of 950 cells/mm^2 [13] and may proliferate into an available space upon meeting the criteria outlined below. Each VSMC has its own unique set of cell variables: damage D, MMP-2 concentration M, ECM density E. An EC monolayer may be added to the lumen surface. The ABM operates in the deformed configuration through importation of nodal displacements from the FE model. The von Mises stress in each VSMC is interpolated from the FE model and used to determine cell damage. Damage causes an upregulation of MMP-2, which decreases ECM density, leading to a change in VSMC phenotype causing cell proliferation. In this work two models which dictate how mechanical damage affects VSMC behaviour are investigated. The models are based on coupled ordinary differential equations, which are outlined in Table 1.

	Model A (Instantaneous Damage)	Model B (Cyclic Damage)
dD/dt	$-k_{deg}^{D}M$	$N \cdot \dot{D} - k_{deg}^{M}M$
dM/dt	$f(D) - k_{deg}^{M}M$	$k_{gen}^{M}D - k_{deg}^{M}M$
dE/dt	$k_{gen}^{E} - k_{deg}^{E}M$	$k_{gen}^{E}\phi - k_{deg}^{M}M$
$d\phi/dt$	$-$	$k_d\{1 - E - \phi\}$
dG/dt	$-$	$k_{gen}^{G}D - k_{deg}^{G}G$
P_{prolif}	Normal Cumulative Distribution: $\mu_{DT} \pm \sigma_{DT}$	$p_{DT} \cdot G \cdot \phi \cdot \Delta t$
Initial Conditions	$D_0 = g(\sigma_{vms})$ $E_0 = E_0$ $M_0 = 0$	$\dot{D} = h(\sigma_{vms})$ $M_0 = 0$ $D_0 = 0$ $\phi_0 = 0$ $E_0 = E_0$ $G_0 = 0$

Table 1: System of coupled ordinary differential equations which determine the response of VSMCs to von Mises stress σ_{vms} for both Model A, based on instantaneous damage, and Model B, based on cyclic damage. The equations prescribe the behaviour for the variables: damage D, MMP-2 concentration M, ECM density E, VSMC phenotype ϕ, growth stimulus G, and probability of a VSMC doubling P_{prolif}. Equation constants assume the format k_a^b where the subscript indicates whether the term causes generation or degradation and the superscript indicates the corresponding variable. Functions $f(D)$ and $g(\sigma_{vms})$ are outlined in [10] and $h(\sigma_{vms})$ in [10].

2.2.1 Model A: Instantaneous Damage

In this case VSMC damage D is determined using a sigmoid function of von Mises stress magnitude ($g(\sigma_{vms})$) which goes from 0 to 1 [10]. Cell phenotype is binary, VSMCs transition from contractile to synthetic when their ECM density falls below 310 pg/cell [15]. Only synthetic VSMCs may proliferate where the probability of doubling is controlled using a normal cumulative distribution which must be calibrated. In this model, proximity to ECs changes VSMC phenotype to a contractile state [16].

2.2.1 Model B: Cyclic Damage

In the cyclic damage model, Miner's Rule ($h(\sigma_{vms})$) is used to calculate damage accumulation in the tissue over time [10]. A damage rate $\dot{D}$ is computed for each VSMC based on its von Mises stress. Damage increases at this rate for every loading cycle N (assumed at 1 Hz here). An endurance limit of 90 kPa is assumed, below which no damage occurs [10]. In addition to MMP-2 and ECM variables this model has a continuous cell phenotype variable ϕ (from contractile to synthetic, 0 to 1), and a growth stimulus variable G. Cell proliferation is controlled by these variables, and the larger the growth stimulus and more synthetic the phenotype, the higher the probability of VSMC doubling.

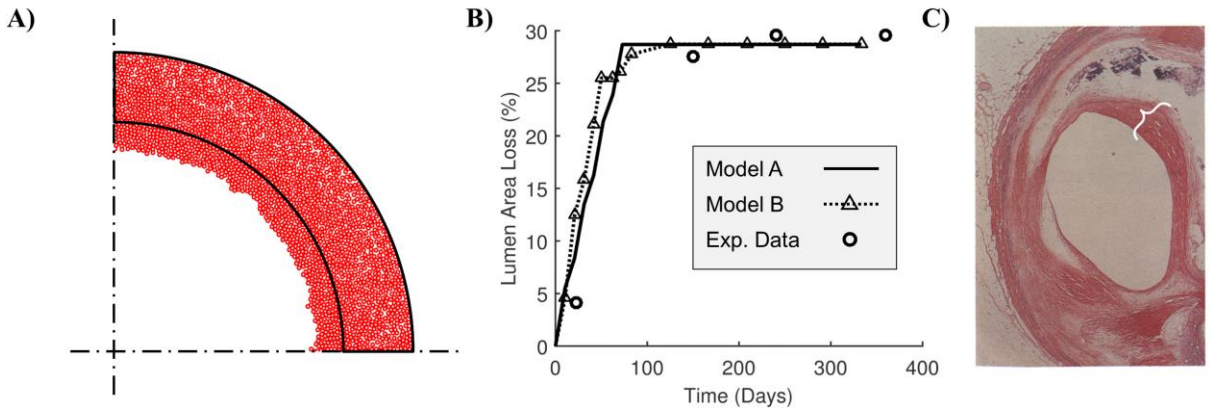

Figure 1: **A)** Resultant stenosis computed by the balloon angioplasty simulation at 350 days. The black outline indicates the artery wall in the initial configuration and red circles indicate the individual VSMCs. Similar stenosis patterns are computed using Models A and B. **B)** Plot of lumen area loss over time determined using Models A and B, compared to the experimentally observed lumen loss presented in Schwartz et al.[6] The balloon angioplasty simulation is used to calibrate the constants for the damage – ECM dynamic equations, see Table 1. **C)** Histological image from [17] of restenosis post balloon angioplasty.

2.3 Simulations

Simulations of balloon angioplasty were performed to calibrate the constants for the equations in Table 1. The internal radius of the artery is expanded to 1.4 times its original size and then returned to physiological pressure. The supra-physiological loading causes damage and induces restenosis. It is assumed that the balloon has denuded the lumen of ECs. Predictions are compared to the clinically measured lumen area loss reported in [13].

The calibrated models are then used to predict in-stent restenosis. A square rigid body representing a stent strut is deployed into the artery wall up to a lumen expansion ratio of 1.2. The simulations using Model A include an EC layer which is assumed to be partially denuded initially. In accordance with [10] simulations using Model B did not include ECs.

3. Results

Fig. 1A shows the setup of the simulations and the result of the balloon angioplasty simulation. VSMCs originally in the media have proliferated into the lumen causing restenosis. Fig. 1B shows lumen area loss with time for both Model A and B alongside the experimental data from [13]. The initial rate of lumen loss is determined strongly by the mean doubling time μ_{DT} for Model A and k_{gen}^{G} and k_{deg}^{G} for Model B. Fig. 2A shows a plot of ECM density change over time for a range of values of initial damage. Recalling that ECM density controls cell phenotype and proliferation in Model A, these curves determine the time at which lumen area loss begins to plateau. Likewise, Fig. 2B plots the probability of VSMC proliferation with time for a range of initial damage values. The time at which this curve reaches its peak will determine the plateau in lumen loss for Model B.

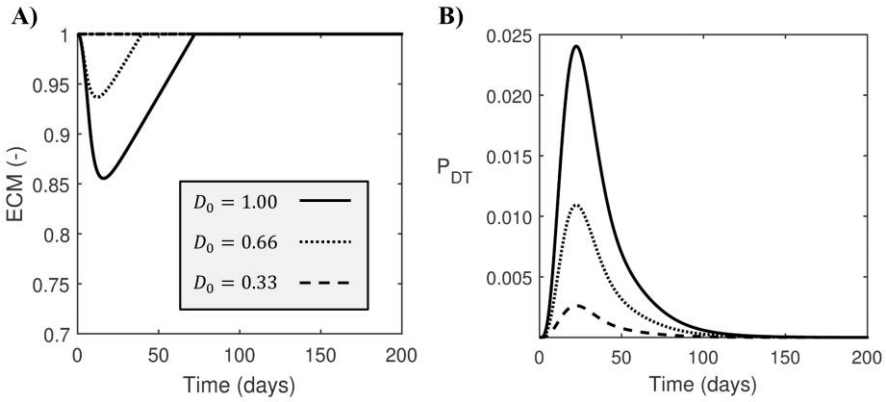

Figure 2: **A)** Plot of normalized ECM density per cell over time for a range of initial values of damage, D_0, for Model A. VSMC phenotype is switched from synthetic to contractile as the ECM transitions from below, to greater than one. Hence this behaviour determines the duration that VSMCs are synthetic and proliferative. **B)** Probability of VSMCs doubling, P_{DT}, for Model B for a range of intial damage values. In this case the duration of cell proliferation is defined by this curve, as the probability of doubling approaches zero.

Results of the stent simulation using Model A are shown in Fig. 3A. There is proliferation of VSMCs around the stent strut where the ECs are initially denuded, this is accompanied by re-endothelialisation of the lumen at 125 days which prevents further proliferation of VSMCs. After deployment of the stent strut, the mean stress in the artery is now above the endurance limit. Hence in Model B there is substantial VSMC proliferation as damage is constantly accumulating (Fig. 3B). At 125 days the Model B predicts that the vessel will be totally occluded.

4. Discussion and Conclusions

The stent simulation using Model A results in predictions of in-stent restenosis patterns similar to those observed clinically and over a similar timeframe [6] (Fig. 3C). The inhomogeneous stress distribution and high mean stress causes Model B to overpredict lumen loss, as there is no stimulus to halt cell proliferation. Though the presence of ECs in Model A aids in the control of VSMC proliferation, the VSMCs will cease to proliferate with time (recall Fig. 2A).

Though the simulations can successfully predict in-stent restenosis, there are limitations to the models. The coupled equations controlling the VSMCs are phenomenological and sensitive to their constants. Future models will incorporate more mechanistic damage – ECM dynamics supported by experimental data. The current framework is also 2D and not fully coupled; as new geometry is computed by the ABM, the FE model should be re-run with this updated geometry.

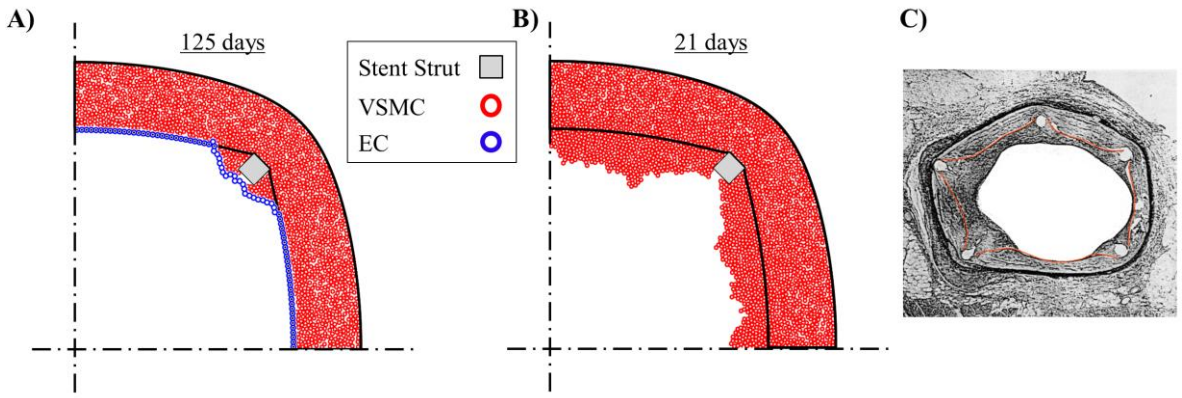

Figure 3: **A)** Response computed at 125 days by the mechanobiological model for simulation of stent deployment using Model A for the damage – ECM dynamics. Note the presence of ECs which cause VSMCs to become contractile when they come within a range of 60 μm. **B)** Response at 21 days of the mechanobiological model using Model B for the damage – ECM dynamics. In this case ECs are not modelled and there is extensive proliferation of cells into the lumen. **C)** Histological image from [18] of in-stent restenosis and neo-intima.

Whilst addressing these limitations in future work, we will also investigate the role of stent strut thickness and the number of struts per cross section on subsequent in-stent restenosis as these parameters are known to considerably affect load induced damage in the artery [19,20]. Finally, we ultimately wish to perform ABM simulations in which collagen fibres are explicitly modelling and can direct cell behaviour. This will allow us to fully test the efficacy of different stent designs at preventing restenosis.

5. References

1. Roger et al., Circ, 2011; 123(e18-e209)
2. Kornowski et al. J Am Coll Cardio 1998; 224
3. Welt et. al., Arterioscler Thromb Vasc Biol., 2002; 22(11):1769–1776
4. Kang et al. Eur. Heart J. 2014: eht570.
5. Kouvelos et al. J Endo. Therap; 2015:789
6. Schwartz et al. J Inter Cardio 1994;7:355-368
7. Thyberg et al., J Histochem Cytochem., 1997;45
8. Newby et al., Cardiovasc Res., 2005; 69:624.
9. Asanuma et al., Am J. Physiol Heart Circ Physiol., 2003; 284:1778–1784
10. Zahedmanesh et al. CMBBE, 2012;1
11. Boyle et al., J Biomech Eng, 2011;133(8)
12. Rouillard et al. Prog. Biophys. Mol. Biol. 2014;115
13. Tracy et al., Virchow Arch. 1997;430:155
14. Schwartz et al. Inter J Cardio 1996;71
15. Hahn et al. Ann. Bio. Eng. 2007;35:190
16. Matsusaki et al. Angew Chem Int Ed 2011;50
17. Nobuyoshi et al, JACC, 1991;433
18. Schwartz et al., J Am Coll Cardiol. 1994; 19:267
19. Zahedmanesh et al. BMMB 2012;11:363
20. Rogers et al. Circ. 1995;91